Output three-mode entanglement via coherently prepared inverted Y-type atoms*

Wang Fei(王 飞)† and Qiu Jing(邱 晶)

College of Science, China Three Gorges University, Yichang 443002, *China*

(Received 23 July 2013; revised manuscript received 31 August 2013; published online 10 February 2014)

In this paper, the output quantum correlations of three fields interacting with inverted Y-type atoms inside a three-mode cavity are investigated. By numerically calculating the stationary noise spectra of the fields, we show that it is possible to generate the genuine tripartite continuous variable entanglement outside the cavity by coherently preparing the atoms in a superposition of the upper excited state and two ground states initially. Our numerical results demonstrate that both zero frequency entanglement and sideband frequency entanglement can be obtained under different initial coherent conditions. In addition, we investigate the thermal fluctuation effects on the quantum entanglement. It is found out that the entanglement occurring in a high frequency regime is more robust against thermal noise than the zero frequency entanglement, which may be useful for quantum communication.

Keywords: tripartite entanglement, correlated spontaneous emission laser, inverted Y-type atom

PACS: 42.50.Dv, 03.65.Ud, 42.50.Lc, 03.67.Bg **DOI:** 10.1088/1674-1056/23/4/044203

1. Introduction

One of the most interesting effects in quantum optics is atomic coherence, which has received much attention due to the fact that it is closely related to a large number of striking phenomena, such as coherent population trapping (CPT),[1] electromagnetically induced transparency (EIT),[2–9] lasing without inversion (LWI),[10–13] the modification of spontaneous emission, etc.[14–17] In recent years, it is shown that atomic coherence plays an important role in generating and manipulating continuous variable (CV) entanglement, which has many advantages in quantum-information science.[18] To date, various schemes are proposed to generate entanglement via atomic coherence effects, such as coherence-induced multi-wave mixing processes,[19–24] one-atom laser,[25–27] quantum-beat laser,[28–30] atomic coherence controlled parametric interaction processes,[31–33] and electromagnetically induced transparency.[34,35] In particular, for a three-level cascade system, the correlated spontaneous emission laser (CEL) has been proposed to act as an entanglement amplifier.[36] Tan *et al*.[37] extended this model, and found that the two-mode field in the cavity can evolve into a two-mode Gaussian state. Zhou *et al*.[38] considered a single three-level cascade atom interacting dispersively with two classical fields. They exhibited that a macroscopic entangled state between these two cavity modes can be generated under large detuning conditions. In the above-mentioned schemes, the atomic coherence is introduced by using strong driving field(s). In addition, there is an alternative way to create atomic coherence by preparing the atoms initially in a coherent superposition. In an early study, Scully and Zubairy[39] presented a theory of two-photon CEL based on a coherently prepared three-level atomic system. On the basis of this theory, Tesfa[40–42] conducted a series of studies of the generation of two-mode squeezing and entanglement.

Recently, Shi *et al*.[43] proposed a scheme for generating tripartite continuous-variable entanglement via three-colored CEL, wherein the atomic coherence is induced by the external strong coherent fields. Later on, by using two strong classical fields to drive a four-level Y-type[44] and an inverted Y-type[45] atomic system, the transient tripartite entanglements were achieved and the entangled period depended strongly on the intensity of the classical fields. In a four-level V-type system, the genuine tripartite entanglement could be achieved via microwave field driven atomic coherence.[46] In fact, the external classical driven fields brought an additional noise, resulting in the absence of steady state entanglement. Very recently, in a four-level Y-type atomic system, Tesfa[47] studied the generation of tripartite entanglement via coherently preparing the atoms in a superposition of the upper two excited energy levels and ground level initially. It is shown that the nondegenerate four-level correlated emission laser can be a source of tripartite entangled light. Although the detailed derivation of the master equation of the cavity radiation was presented there, the analytical results to estimate the tripartite entanglement are difficult to obtain. Accordingly, the quantum correlations of the intracavity fields have just been analyzed qualitatively and the tripartite entanglement has been analyzed briefly. In this paper, we consider an ensemble of four-level inverted Y-type atoms, which is placed inside a three-mode cavity and prepared in a superposition of the upper excited states and two ground

*Project supported by the National Natural Science Foundation of China (Grant Nos. 1137418 and 11104163) and the Science Foundation of Three Gorges University, China (Grant No. KJ2011B019).

†Corresponding author. E-mail: feiwang202@163.com

© 2014 Chinese Physical Society and IOP Publishing Ltd

states initially. With the standard theory proposed by Drummond and Gardiner,[48,49] using the input–output theory[50], we numerically calculate the stationary noise spectra of the fields outside the cavity. Based on the criteria proposed by van Loock and Furusawa,[51] our results demonstrate that the tripartite entanglement can be achieved. Further, when different initial conditions are taken, the output tripartite entanglement can appear not only in the high frequency regime but also at zero frequency. We also note that the degree of the entanglement is enhanced as the linear gain coefficient increases. Besides, the thermal photon effects on the output three-mode entanglement are analyzed numerically. It is found that the thermal noise is harmful for the quantum entanglement. Nevertheless, it is worthwhile to note that the sideband entanglement is much more robust against thermal fluctuations than the zero frequency entanglement. The remainder of this article is organized as follows. In Section 2, we present the model and master equation. In Section 3, the numerical results and discussion are presented. The conclusion is given in Section 4.

2. Model and equations

An ensemble of independent four-level inverted Y-type atoms is placed into a three-mode optical cavity. As illustrated in Fig. 1, by $|1\rangle$ and $|2\rangle$ we denote the two nearly degenerate ground states, $|3\rangle$ is an intermediate energy level, $|4\rangle$ indicates the upper excited state. Three quantized fields of frequencies ω_j ($j=1$–3) are coupled with three dipole allowed transitions, respectively. In the interaction picture, we derive the Hamiltonian as

$$V = \mathrm{i}g\left(a_1\sigma_{31}+a_2\sigma_{32}+a_3\sigma_{43}-a_1^{\dagger}\sigma_{13}-a_2^{\dagger}\sigma_{23}-a_3^{\dagger}\sigma_{34}\right), \quad (1)$$

where the operators $\sigma_{jk}=|j\rangle\langle k|$ ($j,k=1$–3) are the projection operators for $j=k$ and the flip operators for $j\neq k$. $a_j(a_j^{\dagger})$ ($j=1$–3) represent the annihilation (creation) operators of the three cavity modes, g_j ($j=1$–3) are the coupling constants, which are assumed to be real and identical for simplicity.

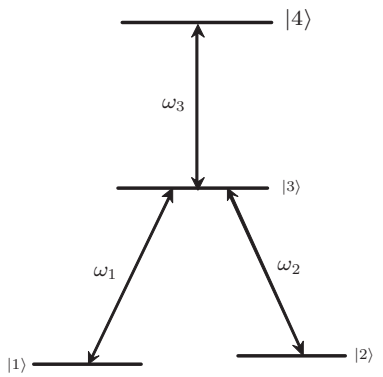


Fig. 1. Energy level structure of the four-level inverted Y-type atom.

We assume that the atoms are initially prepared in the coherent superposition of the atomic levels except the level $|3\rangle$. Then the corresponding initial density operators are

$$\begin{aligned}\rho_A(0) = {} & \rho_{44}^{(0)}|4\rangle\langle 4|+\rho_{22}^{(0)}|2\rangle\langle 2| \\ & +\rho_{11}^{(0)}|1\rangle\langle 1|+\rho_{42}^{(0)}|4\rangle\langle 2| \\ & +\rho_{24}^{(0)}|2\rangle\langle 4|+\rho_{41}^{(0)}|4\rangle\langle 1|+\rho_{14}^{(0)}|1\rangle\langle 4| \\ & +\rho_{21}^{(0)}|2\rangle\langle 1|+\rho_{12}^{(0)}|1\rangle\langle 2|, \end{aligned} \quad (2)$$

where $\rho_{ll}^{(0)}$ ($l=1,2,4$) are the initial populations and $\rho_{lk}^{(0)}$ ($l,k=1,2,4, l\neq k$) are the atomic coherences between different levels.

We take into account the case that the atoms are injected into the cavity with constant rate r_{a} and removed after some time τ. Assuming that the time τ is long enough for the atoms to spontaneously decay to energy levels other than these involved levels.[40–42] Without loss of generality, all decay rates of these levels are assumed to be equal, which are denoted by γ. In the good cavity limit, i.e., $\gamma\gg\kappa$, where κ is the cavity damping constant, the decay rates of the atoms are much faster than that of the cavity, implying that the atomic variables reach a steady state in a short time. Using the adiabatic approximation and the standard linear laser theory, we can obtain the master equation for the cavity fields[52]

$$\begin{aligned}\dot{\rho}_f = {} & \xi_1\left(2a_3^{\dagger}\rho_f a_3-a_3a_3^{\dagger}\rho_f-\rho_f a_3a_3^{\dagger}\right) \\ & +\xi_2\left(2a_1\rho_f a_1^{\dagger}-a_1^{\dagger}a_1\rho_f-\rho_f a_1^{\dagger}a_1\right) \\ & +\xi_3\left(2a_2\rho_f a_2^{\dagger}-a_2^{\dagger}a_2\rho_f-\rho_f a_2^{\dagger}a_2\right) \\ & +\varsigma_1\left(2a_1\rho_f a_2^{\dagger}-a_2^{\dagger}a_1\rho_f-\rho_f a_2^{\dagger}a_1\right) \\ & +\varsigma_1\left(2a_2\rho_f a_1^{\dagger}-a_1^{\dagger}a_2\rho_f-\rho_f a_1^{\dagger}a_2\right) \\ & -\varsigma_2\left(2a_3^{\dagger}\rho_f a_1^{\dagger}-a_1^{\dagger}a_3^{\dagger}\rho_f-\rho_f a_1^{\dagger}a_3^{\dagger}\right) \\ & -\varsigma_2\left(2a_1\rho_f a_3-a_3a_1\rho_f-\rho_f a_3a_1\right) \\ & -\varsigma_3\left(2a_3^{\dagger}\rho_f a_2^{\dagger}-a_2^{\dagger}a_3^{\dagger}\rho_f-\rho_f a_2^{\dagger}a_3^{\dagger}\right) \\ & -\varsigma_3\left(2a_2\rho_f a_3-a_3a_2\rho_f-\rho_f a_3a_2\right) \\ & +\sum_{i=1}^{3}\frac{\kappa_i}{2}\left(2a_i\rho_f a_i^{\dagger}-a_i^{\dagger}a_i\rho_f-\rho_f a_i^{\dagger}a_i\right) \end{aligned} \quad (3)$$

with $\xi_1=A\rho_{44}^{(0)}/2$, $\xi_2=A\rho_{11}^{(0)}/2$, $\xi_3=A\rho_{22}^{(0)}/2$, $\varsigma_1=A\rho_{21}^{(0)}/2$, $\varsigma_2=A\rho_{41}^{(0)}/2$, $\varsigma_3=A\rho_{42}^{(0)}/2$, and $A=2g^2r_a/\gamma$. By defining two parameters: $\eta_1=\rho_{44}^{(0)}-\rho_{11}^{(0)}$, $\eta_2=\rho_{44}^{(0)}-\rho_{22}^{(0)}$, we can obtain the initial populations and atomic coherences based on the fact that $\rho_{11}^{(0)}+\rho_{22}^{(0)}+\rho_{44}^{(0)}=1$ as follows:

$$\begin{aligned} & \rho_{11}^{(0)}=(1-2\eta_1+\eta_2)/3, \quad \rho_{22}^{(0)}=(1+\eta_1-2\eta_2)/3, \\ & \rho_{44}^{(0)}=(1+\eta_1+\eta_2)/3, \quad \rho_{12}^{(0)}=\rho_{21}^{(0)}=\sqrt{\rho_{11}^{(0)}\rho_{22}^{(0)}}, \\ & \rho_{14}^{(0)}=\rho_{41}^{(0)}=\sqrt{\rho_{11}^{(0)}\rho_{44}^{(0)}}, \quad \rho_{24}^{(0)}=\rho_{42}^{(0)}=\sqrt{\rho_{22}^{(0)}\rho_{44}^{(0)}}, \end{aligned} \quad (4)$$

According to Eq. (3), one can readily obtain

$$\frac{\mathrm{d}\langle a_1\rangle}{\mathrm{d}t}=-\left(\frac{1}{2}\kappa_1+\xi_2\right)\langle a_1\rangle-\varsigma_1\langle a_2\rangle+\varsigma_2\left\langle a_3^{\dagger}\right\rangle, \quad (5)$$

$$\frac{\mathrm{d}\langle a_2\rangle}{\mathrm{d}t} = -\left(\frac{1}{2}\kappa_2 + \xi_3\right)\langle a_1\rangle - \varsigma_1\langle a_1\rangle + \varsigma_3\left\langle a_3^{\dagger}\right\rangle, \quad (6)$$

$$\frac{\mathrm{d}\langle a_3\rangle}{\mathrm{d}t} = -\left(\frac{1}{2}\kappa_2 - \xi_1\right)\langle a_3\rangle - \varsigma_2\left\langle a_1^{\dagger}\right\rangle - \varsigma_3\left\langle a_2^{\dagger}\right\rangle, \quad (7)$$

together with those for $a_1^{\dagger}$, $a_2^{\dagger}$, $a_3^{\dagger}$. To investigate the quantum correlation, a standard Langevin approach by means of the generalized P representation is used.[48,49] Choosing the normal order as $a_1^{\dagger}$, $a_2^{\dagger}$, $a_3^{\dagger}$, a_1, a_2, a_3, defining the correspondence between c-number and operators as $\alpha_j \to a_j$, $\alpha_j^* \to a_j^{\dagger}$ ($j = 1$–3), writing $\alpha_j = \langle\alpha_j\rangle + \delta\alpha_j$, we can derive the differential equations for the fluctuations in a compact matrix:

$$\frac{\mathrm{d}\delta\boldsymbol{O}(t)}{\mathrm{d}t} = -M\delta\boldsymbol{O}(t) + \boldsymbol{F}, \quad (8)$$

the column vectors are

$$\delta\boldsymbol{O}(t) = (\delta\alpha_1^*(t), \delta\alpha_2^*(t), \delta\alpha_3^*(t), \delta\alpha_1(t), \delta\alpha_2(t), \delta\alpha_3(t))^{\mathrm{T}}$$

and

$$\boldsymbol{F} = (f_1^*(t), f_2^*(t), f_3^*(t), f_1(t), f_2(t), f_3(t))^{\mathrm{T}}.$$

The fluctuation forces have zero averages $\langle f_x(t)\rangle = 0$ and δ correlations $\langle f_x(t) f_y(t')\rangle = D_{xy}\delta(t-t')$ with $D_{xy} = D_{yx}$, $D_{x^*y^*} = D_{xy}^*$. The drift matrix M and diffusion matrix D can be easily obtained from the Langevin equations. The diffusion matrix D is given as

$$D = \begin{pmatrix} 0 & 0 & \varsigma_2 & 0 & 0 & 0 \\ 0 & 0 & \varsigma_3 & 0 & 0 & 0 \\ \varsigma_2 & \varsigma_3 & 0 & 0 & 0 & 2\xi_1 \\ 0 & 0 & 0 & 0 & 0 & \varsigma_2 \\ 0 & 0 & 0 & 0 & 0 & \varsigma_3 \\ 0 & 0 & 2\xi_1 & \varsigma_2 & \varsigma_3 & 0 \end{pmatrix}. \quad (9)$$

The stationary intracavity correlation spectrum

$$S(\omega) = \int_{-\infty}^{+\infty} \mathrm{e}^{\mathrm{i}\omega\tau}\langle\delta O(t)\,\delta O(t+\tau)\rangle$$

can be derived as

$$S(\omega) = (M + \mathrm{i}\omega I)^{-1} D\left(M^{\mathrm{T}} - \mathrm{i}\omega I\right)^{-1}, \quad (10)$$

where I is a unity matrix.

3. Results and discussion

In this section, we turn to discussing the output quantum correlation of the three cavity modes. To investigate the tripartite entanglement, we define the quadrature operators for each mode as

$$x_j^{\mathrm{o}} = a_j^{\mathrm{o}} + a_j^{\dagger\mathrm{o}}, \quad p_j^{\mathrm{o}} = -\mathrm{i}\left(a_j^{\mathrm{o}} - a_j^{\dagger\mathrm{o}}\right), \quad (11)$$

the superscript "o" indicates the output fields, which are related to the intracavity fields by the input-output relation $a_j^{\mathrm{out}} = \sqrt{\kappa_j}a_j - a_j^{\mathrm{in}}$.[50] Using the criteria for genuine tripartite entanglement proposed by van Loock and Furusawa,[51] the output fields are entangled if any two of the following inequalities are satisfied:

$$\begin{aligned} U_{12} &= V(x_1^{\mathrm{o}} - x_2^{\mathrm{o}}) + V(p_1^{\mathrm{o}} + p_2^{\mathrm{o}} + g_3 p_3^{\mathrm{o}}) < 4, \\ U_{13} &= V(x_1^{\mathrm{o}} - x_3^{\mathrm{o}}) + V(p_1^{\mathrm{o}} + g_2 p_2^{\mathrm{o}} + p_3^{\mathrm{o}}) < 4, \\ U_{23} &= V(x_2^{\mathrm{o}} - x_3^{\mathrm{o}}) + V(g_1 p_1^{\mathrm{o}} + p_2^{\mathrm{o}} + p_3^{\mathrm{o}}) < 4, \end{aligned} \quad (12)$$

where $V(O) = \langle(\delta O)^2\rangle$ and h_j ($j = 1$–3) are arbitrary real parameters that are used to minimize the correlations. The optimization parameters are obtained as $h_1 = -(V_{12} + V_{13})/V_{11}$, $h_2 = -(V_{12} + V_{23})/V_{22}$, $h_3 = -(V_{13} + V_{23})/V_{33}$ with

$$V_{kl} = \frac{1}{2}(\delta p_l \delta p_k + \delta p_k \delta p_l).$$

These values can be obtained via the elements of $S(\omega)$, for instance, $V_{11} = 1 - \kappa[S_{11}(\omega) - S_{14}(\omega) - S_{41}(\omega) + S_{44}(\omega)]$.

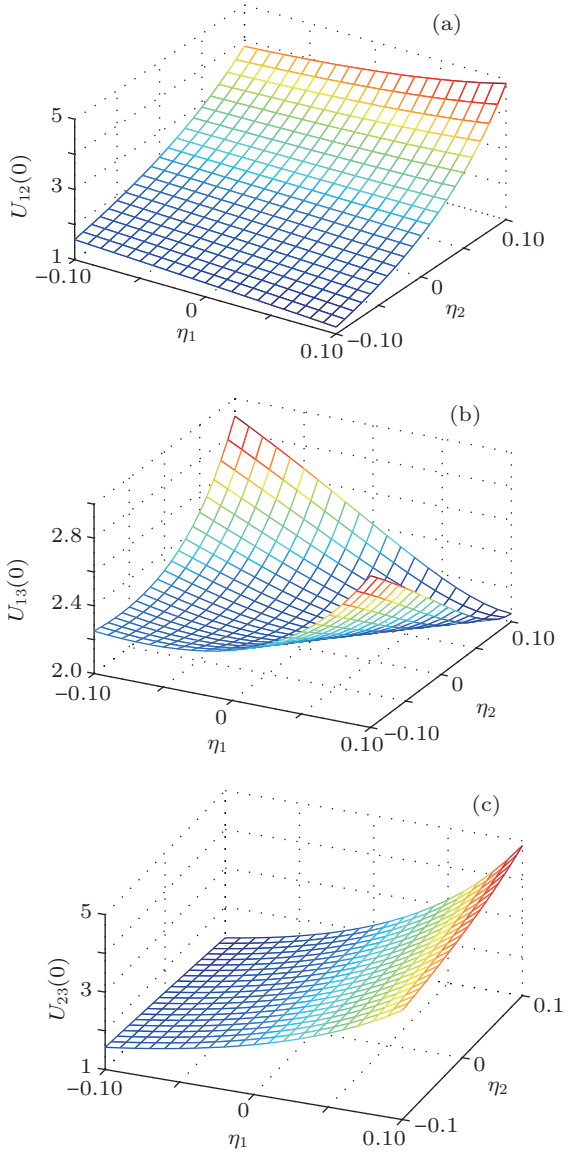


Fig. 2. (color online) Output zero frequency correlation spectra (a) $U_{12}(0)$; (b) $U_{13}(0)$; (c) $U_{23}(0)$ each as a function of η_1 and η_2 for $A = 100$ and $\kappa = 0.2\gamma$.

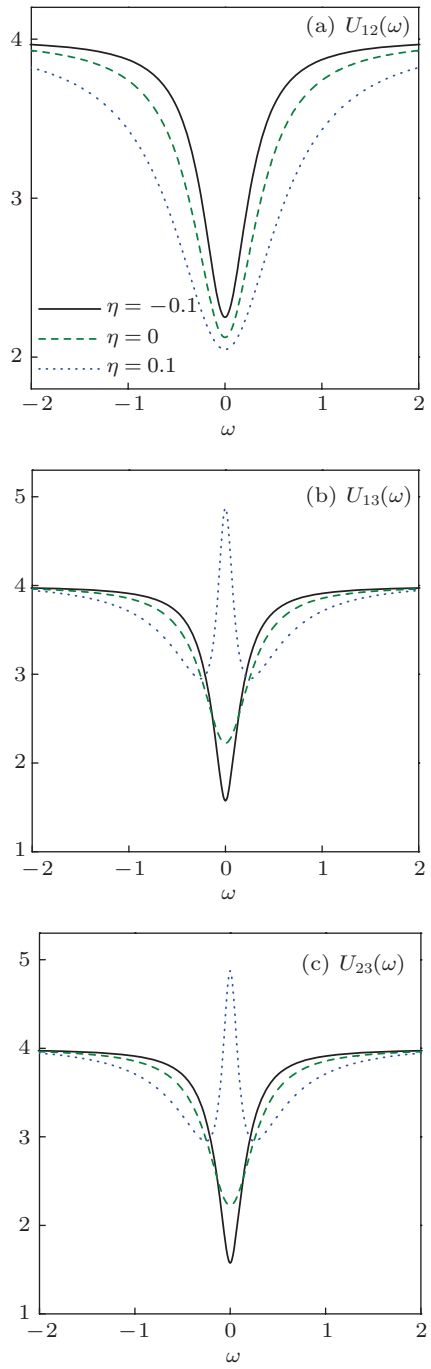


Fig. 3. (color online) Output correlation spectra (a) $U_{12}(\omega)$; (b) $U_{13}(\omega)$; (c) $U_{23}(\omega)$ by choosing the parameters $\eta_1 = \eta_2 = \eta = -0.1$ (solid line), 0 (dashed line), 0.1 (dotted line). The other parameters are the same as those in Fig. 2.

In our numerical calculation, the cavity damping rates, Fourier frequency are scaled in units of γ. Plotted in Fig. 2 are the zero frequency correlation spectra (a) $U_{12}(0)$; (b) $U_{13}(0)$; (c) $U_{23}(0)$ each as a function of η_1 and η_2 in two regions: $-0.1 \leq \eta_1 \leq 0.1$ and $-0.1 \leq \eta_2 \leq 0.1$. Physically, $\omega \to 0$ corresponds to the evolving time of the system $\tau \to \infty$. Therefore, the entanglement generated at the zero frequency means that the steady state entanglement is possible. One should be aware that the range of the two parameters $\eta_{1,2}$ can be beyond the above regions as long as the conditions $0 < \rho_{ii}^{(0)} < 1$, $i = 1,2,4$ are satisfied. The other parameters are chosen as $A = 100$ and $\kappa = 0.2\gamma$. It can be seen clearly that the values of $U_{12}(0)$ are always smaller than 4. However, as shown in Figs. 2(b) and 2(c), the values of $U_{13}(0)$ and $U_{23}(0)$ in some regions are larger than 4. Based on the criteria proposed in Ref. [51], if any two of the three inequalities are satisfied simultaneously, the genuine tripartite entanglement is generated.

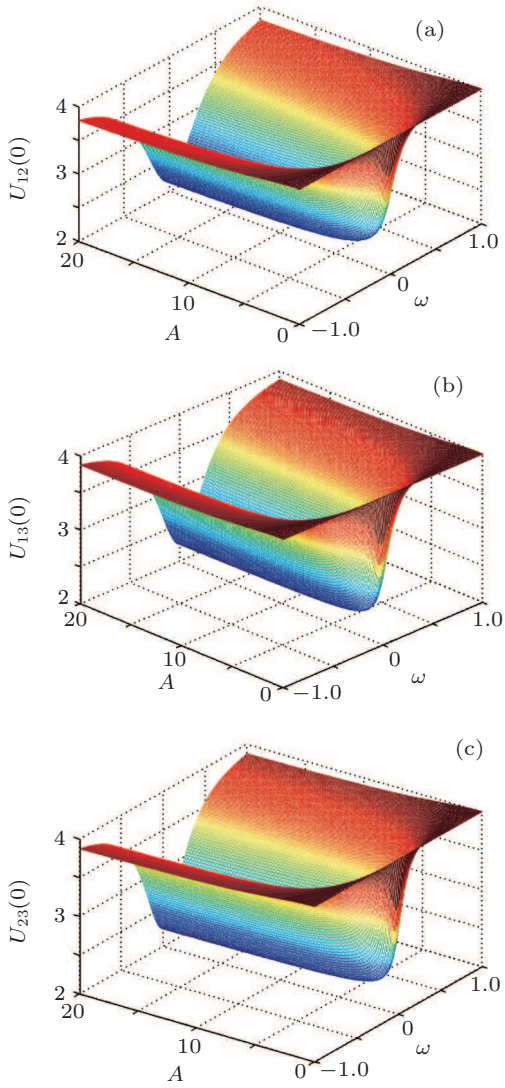


Fig. 4. (color online) Output correlation spectra $U_{ij}(\omega)$ each as a function of A. We take $\eta_{1,2} = 0$, $\kappa = 0.2$.

For a further insight into the characteristics of the present scheme, in Fig. 3, we plot the correlation spectra (a) $U_{12}(\omega)$; (b) $U_{13}(\omega)$; (c) $U_{23}(\omega)$ by taking the parameters $\eta_1 = \eta_2 = \eta = -0.1$ (solid line), 0 (dashed line), 0.1 (dotted line) respectively. The other parameters are the same as those in Fig. 2. When $\eta = -0.1$, the minimal values of the three variances are $U_{12}^{\min}(0) \approx 2.25$, $U_{13}^{\min}(0) \approx 1.57$, and $U_{23}^{\min}(0) \approx 1.57$, implying that the genuine tripartite entanglement is existent not only in the high frequency regime but also at zero frequency. For a special case $\eta = 0$, the initial populations $\rho_{11}^{(0)} = \rho_{22}^{(0)} = \rho_{44}^{(0)} = 1/3$, which corresponds to a maximum initial atomic coherence. In this case, the correlation characteristics are similar to those in the above case. However,

with the parameters changing to $\eta = 0.1$, the correlation values for $U_{13}(0)$ and $U_{23}(0)$ are much larger than 4. This means the absence of the tripartite entanglement at zero frequency. On the other hand, in the high frequency regime, the correlation values of the three variances are less than 4 and the minimal values for the three variances are $U_{12}^{\min}(0) \approx 2.04$, $U_{13}^{\min}(\pm 0.26) \approx 2.95$, $U_{23}^{\min}(\pm 0.26) \approx 2.95$. Accordingly, the tripartite entanglement in this case is existent in the high frequency regime but is absent at zero frequency.

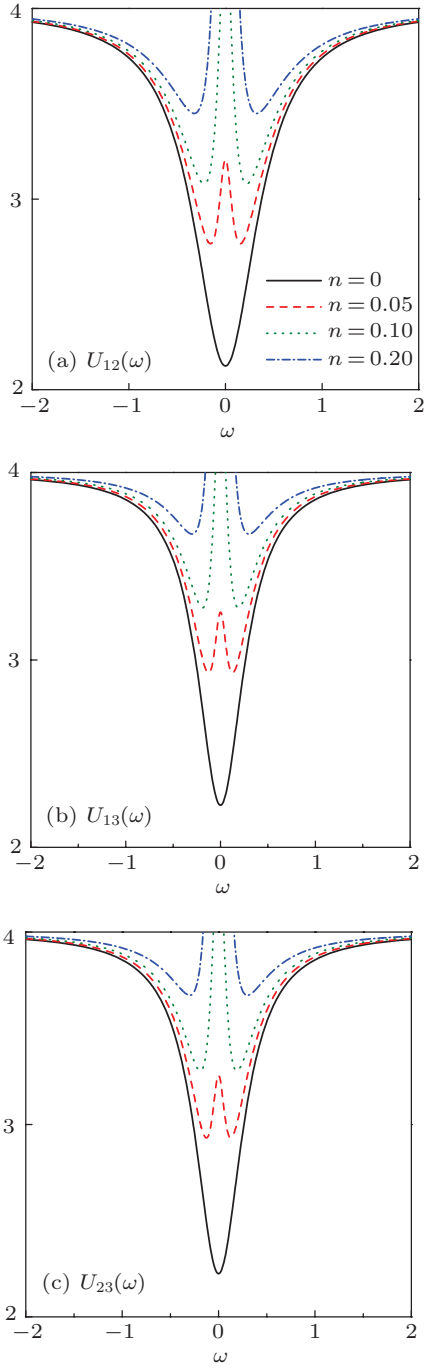


Fig. 5. (color online) Output correlation spectra for $n_j = n = 0$ (solid line), 0.05 (dashed line), 0.10 (dotted line), 0.2 (dash–dotted line). The other parameters are chosen as $A = 100$, $\kappa = 0.2\gamma$, and $\eta_{1,2} = 0$.

In Fig. 4, we show the dependences of correlation spectra $U_{ij}(\omega)$, $ij = 12, 13, 23$ on linear gain coefficient A. The parameters $\eta_{1,2}$ are set to be $\eta_{1,2} = 0$; the cavity damping rates are chosen as $\kappa = 0.2$. Evidently, it is seen that all of the three variances are below 4 even when A is near to zero. As the linear gain coefficient A increases, all of the three correlation values are reduced. The enhancement of tripartite entanglement is achievable.

Next, we discuss the thermal photon fluctuation effects on the quantum entanglement. Using the standard reservoir theory, an additional term should be added to the cavity damping rates[53]

$$\mathcal{L}\rho = \sum_{i=1}^{3} \frac{\kappa_j}{2} n_j \left(2a_j \rho_f a_j^{\dagger} - a_j^{\dagger} a_j \rho_f - \rho_f a_j^{\dagger} a_j\right) + \sum_{i=1}^{3} \frac{\kappa_j}{2} n_j \left(2a_j^{\dagger} \rho_f a_j - a_j a_j^{\dagger} \rho_f - \rho_f a_j a_j^{\dagger}\right), \quad (13)$$

where n_j ($j = 1$–3) are the mean photon numbers for each mode a_j. In Fig. 5, we plot the correlation spectra $U_{ij}(\omega)$, $ij = 12, 13, 23$ for different mean photon numbers $n_j = n = 0$ (solid line), 0.05 (dashed line), 0.10 (dotted line), 0.2 (dash–dotted line). From this figure, we can find that the values of the correlation spectra rise as the photon number increases. Particularly, the values at zero frequency are increased sharper than those at the sideband. Therefore, the thermal fluctuations spoil the steady state tripartite quantum entanglement. In sharp contrast to that, in the high-frequency regime, one can obtain $U_{12}^{\min}(\pm 0.32) \approx 3.45$, $U_{13}^{\min}(\pm 0.32) = U_{23}^{\min}(\pm 0.32) \approx 3.67$ even for $n = 0.2$. Thus, although the thermal noise is harmful for the desired quantum correlation, the entanglement in the high frequency region is robust against the thermal noise.

Before ending this section, we analyze the correlation mechanisms of the present system briefly. First of all, in the two independent cascading transitions from the top state to the two lower ground states, a photon represented by a_3 is emitted from state $|4\rangle$ to intermediate state $|3\rangle$. Successively, it follows a direct emission through two different channels $|3\rangle \to |1\rangle$ or $|3\rangle \to |2\rangle$. As a result, the correlations between modes (a_3, a_1) and (a_3, a_2) are established, which can be attributed essentially to the coherence preparing between the top state and ground states initially. In addition, since there exists a coherence between two ground states $|2\rangle$ and $|1\rangle$, a quantum-beat between modes a_1 and a_2 is created, bringing forth the correlation between them. In a word, any two of the three modes are correlated with each other and the genuine tripartite entanglement occurs. Finally, in comparison with previous schemes, the present system has main differences as follows. On the one hand, as shown in Refs. [43]–[46], the three-mode entanglement is generated within a certain time via atomic coherence induced by the external strong driving field. Due to the fact that additional thermal fluctuations are raised by introducing external pumping fields, one cannot obtain the steady state entanglement. Nevertheless, in the present scheme, we show

that the tripartite entanglement can be generated not only at zero frequency but also at the sideband under different initial conditions. On the other hand, it has been reported recently that a coherently prepared nondegenerate Y-shaped four-level correlated emission laser can be used as a source of tripartite entangled light. For the Y-type and inverted Y-type four-level atoms, the difference mainly lies in the fact that the atomic coherence effects on the two-photon processes are different from each other, which has been proved in Refs. [54] and [55]. Besides, in the present scheme, the EIT can be induced more easily than that in the Y-type system. Although the procedure to achieve the master equation has been presented in detail in Ref. [47], owing to the fact that one can solve the analytical results hardly, the tripartite entanglement has just been analyzed briefly. In this paper, the main innovative points are listed as follows.

(i) We calculate the output sum variances to detect the tripartite entanglement via the stationary noise spectrum.

(ii) Our numerical results show that the tripartite entanglement can be obtained at zero frequency and the sideband frequency for different initial coherent conditions. Besides, we exhibit that the degree of tripartite entanglement is strongly dependent on the linear gain coefficient and cavity damping rate.

(iii) The thermal photon effect on the quantum entanglement is discussed. It is explored that although the larger thermal photons spoil the zero frequency quantum entanglement, good tripartite entanglement is still achievable in a high-frequency regime, which may be useful for the long-distance quantum communications.

4. Conclusion

In this paper, we studied the output quantum correlations of the three quantized fields interacting with four-level inverted Y-type atoms via calculating the stationary noise spectrum numerically. Owing to the fact that the atoms are prepared in a superposition of the upper excited state and the two lower ground states, the three modes outside the cavity are correlated with each other, giving rise to the occurrence of the genuine tripartite entanglement. Our numerical results demonstrate that the entanglement can be obtained not only in a high frequency regime but also at zero frequency under different conditions. Moreover, the dependence of the tripartite entanglement on the linear gain coefficient together with the thermal photon effects is also discussed.

References

[1] Arimondo E 1996 *Progress in Optics* (Amsterdam: Elsevier Science)
[2] Harris S E 1997 *Phys. Today* **50** 36
[3] Marangos J P 1998 *J. Mod. Opt.* **45** 471
[4] Lukin M D and Imamoglu A 2001 *Nature* **413** 273
[5] Lukin M D 2003 *Rev. Mod. Phys.* **75** 457
[6] Fleischhauer M, Imamoglu A and Marangos J P 2005 *Rev. Mod. Phys.* **77** 633
[7] Wu Y, Saldana J and Zhu Y F 2003 *Phys. Rev. A* **67** 013811
[8] Wu Y and Yang X X 2005 *Phys. Rev. A* **71** 053806
[9] Yang H, Yang D, Zhang M, Fang B, Zhang Y and Wu J H 2012 *Chin. Phys. B* **21** 114207
[10] Imamoglu A 1989 *Phys. Rev. A* **40** 2835
[11] Zhu S Y and Fill E E 1990 *Phys. Rev. A* **42** 5684
[12] Scully M O 1992 *Phys. Rep.* **219** 191
[13] Mandel P 1993 *Contemp. Phys.* **34** 235
[14] Zhu S Y and Scully M O 1996 *Phys. Rev. Lett.* **76** 388
[15] Paspalakis E and Knight P L 1998 *Phys. Rev. Lett.* **81** 293
[16] Keitel C H 1999 *Phys. Rev. Lett.* **83** 1307
[17] Hu X M, Shi W X, Xu Q, Guo H J and Li J Y 2006 *Phys. Lett. A* **352** 543
[18] Braunstein S L and van Look P 2005 *Rev. Mod. Phys.* **77** 513
[19] Li G X, Tan H T and Macovei M 2007 *Phys. Rev. A* **76** 053827
[20] Wu Y, Payne M G, Hagley E W and Deng L 2004 *Phys. Rev. A* **69** 063803
[21] Pielawa S, Morigi G, Vitali D and Davidovich L 2007 *Phys. Rev. Lett.* **98** 240401
[22] Cheng G L, Hu X M, Zhong W X and Li Q 2008 *Phys. Rev. A* **78** 33811
[23] Shi W X, Hu X M, Li J Y and Wang F 2010 *J. Phys. B: At. Mol. Opt. Phys.* **43** 155506
[24] Chen G L, Chen A X and Zhong W X 2011 *Opt. Commun.* **284** 4028
[25] Morigi G, Eschner J, Mancini S and Vitali D 2006 *Phys. Rev. Lett.* **96** 023601
[26] Lü X Y, Liu J B, Si L G and Yang X X 2008 *J. Phys. B: At. Mol. Opt. Phys.* **41** 035501
[27] Kiffner M, Zubairy M S, Evers J and Keitel C H 2007 *Phys. Rev. A* **75** 033816
[28] Qamar S, Ghafoor F, Hillery M and Zubairy M S 2008 *Phys. Rev. A* **77** 062308
[29] Qamar S, Al-Amri M, Qamar S and Zubairy M S 2009 *Phys. Rev. A* **80** 033818
[30] Hao X Y, Lü X Y, Liu L and Yang W X 2009 *J. Phys. B: At. Mol. Opt. Phys.* **42** 105502
[31] Liang X, Hu X M and He C 2012 *Phys. Rev. A* **85** 032329
[32] Li X and Hu X M 2013 *Laser Phys. Lett.* **10** 075202
[33] Zhang X, Hu X M, Zhang X H and Wang F 2010 *Chin. Phys. B* **19** 124204
[34] Dantan A, Cviklinski J, Giacobino E and Pinard M 2006 *Phys. Rev. Lett.* **97** 023605
[35] Wang F, Hu X M, Shi W X and Zhu Y Y 2010 *Phys. Rev. A* **81** 033836
[36] Xiong H, Scully M O and Zubairy M S 2005 *Phys. Rev. Lett.* **94** 023601
[37] Tan H T, Zhu S Y and Zubairy M S 2005 *Phys. Rev. A* **72** 022305
[38] Zhou L, Xiong H and Zubairy M S 2006 *Phys. Rev. A* **74** 022321
[39] Scully M O and Zubairy M S 1987 *Phys. Rev. A* **35** 752
[40] Tesfa S 2006 *Phys. Rev. A* **74** 043816
[41] Tesfa S 2008 *Phys. Rev. A* **77** 013815
[42] Tesfa S 2009 *Phys. Rev. A* **79** 033810
[43] Shi W X, Hu X M and Wang F 2009 *J. Phys. B: At. Mol. Opt. Phys.* **42** 165506
[44] Lü X Y, Huang P, Yang W X and Yang X X 2009 *Phys. Rev. A* **80** 032305
[45] Song P J, Hao X Y, Huang P and Zhan Z M 2010 *Opt. Commun.* **283** 2982
[46] Jin L X, Lü X Y, Song P J and Yang X X 2010 *Chin. Phys. Lett.* **27** 040310
[47] Tesfa S 2011 *Phys. Rev. A* **83** 052322
[48] Drummond P D and Gardiner C W 1980 *J. Phys. A: Math. Gen.* **13** 2353
[49] Drummond P D and Walls D F 1981 *Phys. Rev. A* **23** 2563
[50] Gardiner C W and Zoller P 2000 *Quantum Noise* (Berlin: Springer)
[51] van Loock P and Furusawa A 2003 *Phys. Rev. A* **67** 052315
[52] Louisell W H 1973 *Quantum Statistical Properties of Radiation* (New York: Wiley)
[53] Scully M O and Zubairy M S 1997 *Quantum Optics* (Cambridge: Cambridge University Press)
[54] Agarwal G S and Harshawardhan 1996 *Phys. Rev. Lett.* **77** 1039
[55] Yan M, Rickey E G and Zhu Y F 2001 *Phys. Rev. A* **64** 043807